The Arp2/3 complex has essential roles in vesicle trafficking and transcytosis in the mammalian small intestine

Kang Zhou, Kaelyn D. Sumigray, and Terry Lechler
Department of Dermatology and Department of Cell Biology, Duke University Medical Center, Durham, NC 27710

ABSTRACT The Arp2/3 complex is the only known nucleator of branched F-actin filaments. Work in cultured cells has established a wide array of functions for this complex in controlling cell migration, shape, and adhesion. However, loss of Arp2/3 complex function in tissues has yielded cell type–specific phenotypes. Here we report essential functions of the Arp2/3 complex in the intestinal epithelium. The Arp2/3 complex was dispensable for intestinal development, generation of cortical F-actin, and cell polarity. However, it played essential roles in vesicle trafficking. We found that in the absence of ArpC3, enterocytes had defects in the organization of the endolysosomal system. These defects were physiologically relevant, as transcytosis of IgG was disrupted, lipid absorption was perturbed, and neonatal mice died within days of birth. These data highlight the important roles of the Arp2/3 complex in vesicle trafficking in enterocytes and suggest that defects in cytoplasmic F-actin assembly by the Arp2/3 complex, rather than cortical pools, underlie many of the phenotypes seen in the mutant small intestine.

INTRODUCTION

The intestinal epithelium consists largely of highly polarized columnar cells called enterocytes. These cells have dual functions in nutrient absorption and in the formation of a barrier against the contents of the intestinal lumen. Hallmarks of these cells include a distinct apical surface covered with microvilli, apical junctional complexes that allow adhesion and barrier formation, and an elongated shape. All of these characteristics are believed to depend on the F-actin cytoskeleton. Perturbation of proteins that assemble, disassemble, and organize F-actin has been a valuable tool in understanding their functions in cell culture. To date, there have been only a few instances in which this type of analysis has been extended to the small intestinal epithelium. For example, the F-actin–binding protein ezrin is important for assembly of the terminal web, an F-actin–rich region underlying microvilli. Furthermore, loss of ezrin results in villus morphology defects (Saotome *et al.*, 2004). Type I myosins have been shown to play roles in localization of brush border enzymes and generation of vesicles from the tips of microvilli (Tyska and Mooseker, 2004; Tyska *et al.*, 2005; McConnell *et al.*, 2009). However, there has been no characterization of the effect of loss of F-actin nucleators, including formins and the Arp2/3 complex, in the intestine. Although formins and other WH2 domain–containing proteins generate linear F-actin actin arrays, the Arp2/3 complex is the only known branched actin nucleator (Pollard, 2007).

Although work in cultured cells has established myriad functions of the Arp2/3 complex (Rotty *et al.*, 2013), genetic studies in intact organisms have revealed cell type–specific roles. For example, RNA interference (RNAi) depletion of Arp2/3 complex components in the *Caenorhabditis elegans* gut resulted in a decrease in apical F-actin and some apically associated proteins, such as ezrin, consistent with its canonical role in generating cortical F-actin (Bernadskaya *et al.*, 2011). However, in a variety of tissue contexts, loss of Arp2/3 complex activity resulted in unexpected phenotypes. In *Drosophila* sensory organ precursor cells, Arp2/3 complex loss of function resulted in Notch signaling defects due to loss of proper targeting of vesicles that contain the Notch ligand, Delta (Rajan *et al.*, 2009). In mammalian epidermis, loss of Arp2/3 complex activity resulted in tight junction defects and overactivation of the Yap1 pathway, driving hyperproliferation and differentiation defects (Zhou *et al.*, 2013).

Finally, genetic studies in the brain demonstrated that the Arp2/3 complex was important for structural plasticity and long-term maintenance of F-actin–rich dendritic spines, leading to schizophrenia-like phenotypes (Kim et al., 2013). These data highlight the diverse roles that the Arp2/3 complex plays in tissue physiology and demonstrate that its functional roles cannot be predicted based exclusively on work in cultured cells.

The Arp2/3 complex requires activation by nucleation-promoting factors (NPFs; Firat-Karalar and Welch, 2011; Rotty et al., 2013). Most of these are involved in generating cortical F-actin in response to external stimuli (e.g., N-WASP and WAVE). However, the NPF WASH has been localized to cytoplasmic vesicles, and depletion of WASH leads to vesicle-trafficking defects (Derivery et al., 2009; Gomez and Billadeau, 2009; Duleh and Welch, 2010, 2012; Gomez et al., 2012). Consistent with this, defects in vesicle trafficking have been reported in both cultured cells and Drosophila sensory organ precursors upon loss of Arp2/3 complex activity (Rajan et al., 2009; Duleh and Welch, 2010, 2012). In addition, the Arp2/3 complex is required for endocytosis in yeast, although its role in endocytosis in mammalian cells is more complex (Galletta and Cooper, 2009). In intact mammalian tissues, a role for the Arp2/3 complex in vesicular organization or trafficking has not been reported, and it is unclear what, if any, cell types require Arp2/3 complex activity for these functions.

Here we show that loss of the Arp2/3 complex component ArpC3 in the mouse small intestine causes early postnatal lethality. Strikingly, the intestine did not exhibit defects in cell shape, polarity, adhesion, or cortical F-actin, but we report that the proper morphology of cytoplasmic vesicles, including the endolysosomal system, is disrupted. Both transcytosis of immunoglobulin G (IgG) across the cell and jejunal absorption of lipids are impaired. These data highlight an important role for the Arp2/3 complex in regulating vesicle trafficking in enterocytes.

RESULTS
Loss of ArpC3 in the intestinal epithelium results in failure to thrive and lethality
To investigate the role of the Arp2/3 complex in the gut, we generated Villin-Cre;ArpC3fl/fl mice (referred to here as ArpC3 cKO). Villin-Cre is expressed throughout the intestinal epithelium starting at midgestation (Madison et al., 2002). ArpC3 is a component of the Arp2/3 complex and is required for robust F-actin nucleation activity (Gournier et al., 2001). In the absence of ArpC3, the Arp2/3 complex's nucleation activity is reduced 10-fold and its in vivo localization is perturbed (Gournier et al., 2001; Zhou et al., 2013). Although an intact complex can be generated in the absence of ArpC3 in vitro, the complex is destabilized in cell extracts (Winter et al., 1999; Gournier et al., 2001). Work in the mouse epidermis and brain demonstrated an essential role for ArpC3 in tissue function and, in Listeria monocytogenes, motility within cells (Kim et al., 2013; Zhou et al., 2013). Therefore loss of ArpC3 likely reflects a substantial but not complete loss of Arp2/3 complex activity.

At birth, ArpC3 cKO pups were indistinguishable from their wild-type littermates by gross outward appearance and body weight (Figure 1C and unpublished data). We confirmed that the ArpC3 protein was lost in mutant pups by isolating intestinal epithelial cells and performing Western blot analysis (Figure 1A). Histological analysis of mutant newborns by hematoxylin and eosin staining revealed a normal gut architecture (Figure 1, G and H). This was confirmed by staining cryosections with anti–α-catenin antibodies to highlight epithelial architecture (Fig 1, I and J). Villi formed and were of comparable length to controls, and cell shape was normal (Figure 1, K

and L). We also did not note any disruption in colon architecture or cell shape (Figure 1, M and N, and unpublished data). These data demonstrate that ArpC3 is not required for neonatal intestinal development, the transition from pseudostratified to simple epithelium, or formation of villi.

In contrast, the postnatal development of ArpC3 cKO mice was severely impaired. By postnatal day 2 (P2), the average body weight of ArpC3 cKO mice was ~70% of that of wild-type littermates (Figure 1, B and D), although they were equivalent at P0 (Figure 1C). We measured intestinal length and similarly found that the length of the ArpC3 cKO intestine was significantly shorter than the wild type at P2 and not at P0 (Figure 1, E and F), consistent with the growth defect. The shorter intestine was proportional to body mass and therefore likely reflects the failure to grow rather than a specific intestinal defect. Most pups died within 2–3 d of birth. For analysis of the underlying cause of these phenotypes, we used neonates taken early on P0 to avoid secondary defects that could result from their failure to thrive. Unless otherwise indicated, images shown are from the jejuna of control and mutant mice.

ArpC3 cKO mice have no gross defects in F-actin organization
In the C. elegans intestine, RNAi knockdown or mutation of Arp2/3 complex components or its activators alters filamentous actin (F-actin) organization (Bernadskaya et al., 2011). To determine whether F-actin organization was notably disrupted in the mutant, we stained intestinal sections with fluorescent phalloidin. Surprisingly, we did not observe gross changes in cortical F-actin in the mutant intestine (Figure 2, A and B). Phalloidin strongly labeled the brush border in both wild-type and ArpC3 cKO mice, and quantitation of fluorescence intensity demonstrated that the ArpC3 cKO was not significantly different from the wild type (Figure 2C). Whereas the brush border has the highest concentration of F-actin, the basolateral membrane also has an enrichment. There was no difference in intensity or organization of F-actin at these lateral sites when longer exposures were used (Figure 2, A', B', and C). Consistent with these data, electron microscopy of ultrathin sections revealed that microvilli were normal in appearance (Figure 2, D and E). Other F-actin structures within the cytoplasm and fine details of cortical actin organization cannot be discerned by traditional light microscopy techniques. That said, our data demonstrate that ArpC3 is not required for the generation of the bulk of cortical F-actin within the enterocyte.

Loss of ArpC3 does not disrupt cell–cell adhesion or polarity
Studies in cultured cells and the Drosophila notum have demonstrated a requirement for Arp2/3 complex activity in actin assembly at the adherens junction (Verma et al., 2004, 2012; Georgiou et al., 2008; Tang and Brieher, 2012). In contrast, mouse epidermal adherens junctions appeared normal upon loss of Arp2/3 complex activity, although tight junction defects were apparent (Zhou et al., 2013). To determine whether a simple mammalian epithelium in situ requires Arp2/3 complex activity for proper apical junction formation, we assessed the ultrastructural organization of apical cell–cell contacts. In both wild-type (WT) and ArpC3 cells, we observed membrane appositions representing tight junctions, electron-dense desmosomes, and less-defined adherens junctions between them (Figure 2, F and G). To determine the localization of cell–cell adhesion proteins, we immunostained neonatal WT and ArpC3 cKO mice for E-cadherin, the major canonical cadherin in the small intestine. We observed normal lateral localization of E-cadherin with similar intensity in both WT and mutant enterocytes (Figure 2, H and I). Similarly, the adherens junction protein α-catenin was normally
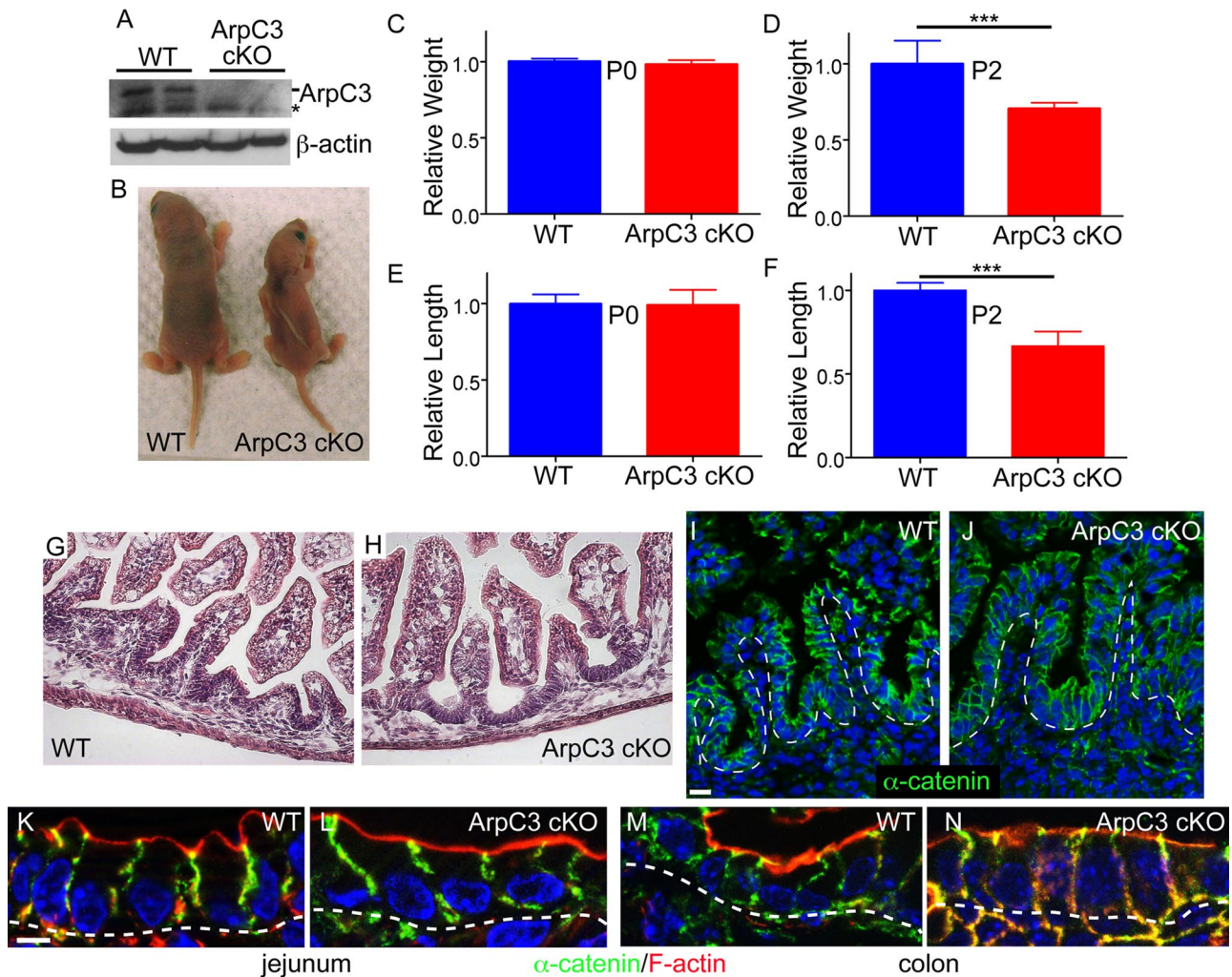
FIGURE 1: Normal intestinal architecture but failure to thrive upon loss of ArpC3 in the intestinal epithelium. (A) Western blots for ArpC3 and actin in extracts prepared from two WT and two ArpC3 cKO pups. (B) WT and ArpC3 cKO littermates at postnatal day 2. (C–F) Relative weights of P0 and P2 pups, as well as the relative intestinal lengths at these two time points. WT weight and intestinal length was set to 1 in each case. $n = 7$ or 8, $p < 0.0001$ for both. (G, H) Hematoxylin and eosin staining of neonatal WT and ArpC3 cKO jejuna. Scale bar, 50 μm. (I, J) α-Catenin (green) and nuclei (blue) in WT and ArpC3 cKO jejuna. Scale bar, 20 μm. Dotted lines indicate basement membrane. (K–N) α-Catenin (green) and F-actin (red) in WT and ArpC3 jejuna (K, L) and colon (M, N). Nuclei are blue; dotted lines indicate the basement membrane. Scale bar, 10 μm.

localized (Figure 1, K and L). E-cadherin was restricted to the lateral domain and was not present on the apical surface. We also examined the localizations of the tight junction proteins ZO-1 and occludin, which demarcate the apical/basolateral boundary. In WT intestine, ZO-1 and occludin were enriched at apical puncta when viewed from the side (Figure 2, H and J). This same pattern of localization was found in the mutant intestine (Figure 2, I and K). However, we also examined ZO1 localization in whole-mount epithelia rather than sections in order to see the apical surface *en face*. Using this imaging method, we noticed a slightly less regular pattern of staining and a small increase in cytoplasmic puncta of ZO1 (Figure 2, L and M). In addition, in a small number of villi, we noted that the regular hexagonal shapes of the apical cell surface was disrupted (Figure 2, N and O). These data demonstrate that Arp2/3 complex function is largely dispensable for tight junction protein localization in the small intestine. Of note, cell adhesion function is distinct from localization, and our assays do not address whether junctional turn-over or junctional tension is affected in the mutant. Indeed, the low level of apical disorganization that we observed might underlie defects in apical tension in these cells.

Next we investigated whether cell polarity was disrupted by examining the localization of ezrin, a cytoplasmic protein that associates with the apical membrane. It localized normally with a similar intensity in ArpC3 cKO and control mice (Figure 2, P and Q), in contrast to the *C. elegans* intestine where ezrin localization was dependent upon the Arp2/3 complex (Bernadskaya *et al.*, 2011). Moreover, the *trans*-Golgi network marker Grasp64 localized to the top of the nucleus facing the apical domain in both wild-type and mutant intestine (Figure 2, R and S). We did not detect any evidence of fragmentation of the *trans*-Golgi network in ArpC3 cKO mice. Myosin 1d, which marks both the terminal web and brush border, also showed normal localization in the mutant (Figure 2, T and U). Taken together, these results demonstrated that cell adhesions and cell polarity are not dramatically altered upon loss of Arp2/3 complex function.
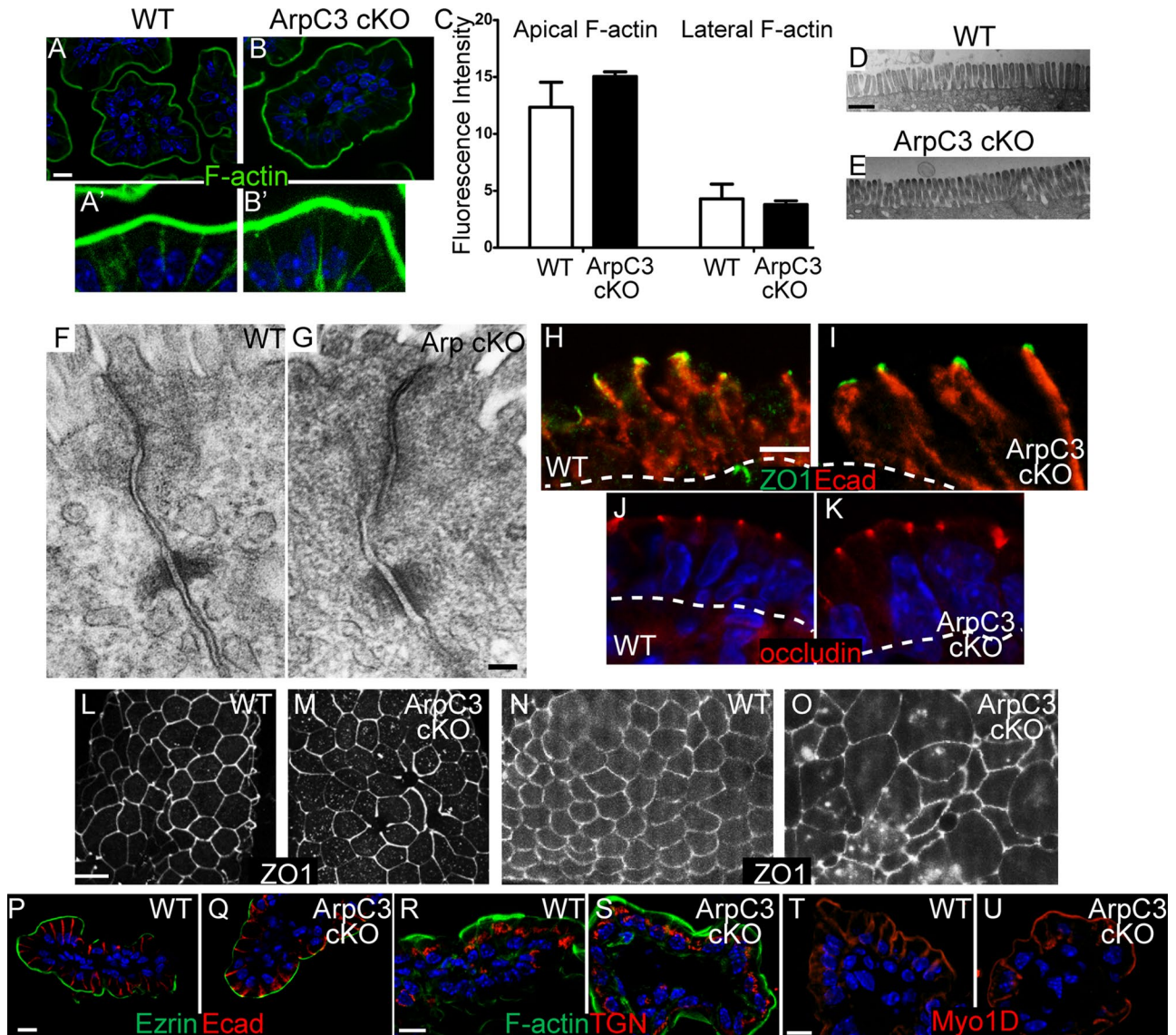
FIGURE 2: Normal cortical F-actin, polarity, and adhesion in ArpC3 cKO mice. (A–B') F-actin staining of WT (A) and ArpC3 cKO (B) intestinal sections. A' and B' are brightness enhanced to visualize the low levels of lateral F-actin. (C) Quantitation of fluorescence intensity of phalloidin staining of F-actin. (D, E) Transmission electron micrographs of the brush borders of WT and ArpC3 cKO intestine. Scale bar, 2 10 μm. (F, G) Transmission electron micrographs of the apical junctions of WT and ArpC3 cKO intestine. (H, I) Tight junction (ZO-1, green) and adherens junctions (E-cadherin, red) staining in WT and ArpC3 cKO intestine. Scale bar, 10 μm. Dashed line indicates the basement membrane. (J, K) Occludin (red) localization in WT and ArpC3 cKO intestine. (L–O) Whole-mount intestines stained for ZO1. L–N represent the predominant phenotype, and O represents the status of ZO1 in a smaller number of mutant villi. (P, Q) Ezrin (green) and E-cadherin (red) staining of WT and mutant intestine. (R, S) WT and mutant intestinal sections were stained for the *trans*-Golgi network protein, Grasp64 (red) and F-actin (green). (T, U) Staining for the terminal web and brush border marker myosin 1D (red) in WT and ArpC3 cKO intestine. Scale bars, 10 μm.

ArpC3 cKO intestines exhibit normal proliferation and differentiation

In some tissues, loss of the Arp2/3 complex has unexpected phenotypes, such as affecting proliferation and differentiation (Rajan *et al.*, 2009; Zhou *et al.*, 2013). To determine whether this was the case in the intestine, we stained intestinal sections with antibodies against the proliferation marker Ki67. As in the wild type, Ki67 expression was restricted to the intervillar regions in ArpC3 cKO mice (crypts develop postnatally and are not present at this stage). Quantitation of the number of Ki67-positive cells within these regions revealed no statistically significant difference (Supplemental Figure S1).

Furthermore, we did not observe an appreciable amount of apoptosis in either wild-type or ArpC3 cKO intestine by active-caspase 3 staining (unpublished data). Finally, the Arp2/3 complex regulates Notch signaling in the *Drosophila* sensory organ precursor (Rajan *et al.*, 2009). In the gut, Notch signaling controls goblet cell differentiation (van Es *et al.*, 2005). However, we did not detect any changes in the number of goblet cells in the mutant intestine (Supplemental Figure S1), suggesting that Arp2/3 complex activity does not regulate Notch signaling in this tissue. Therefore neonatal lethality is not related to defects in proliferation, differentiation, or cell type specification.

Vesicle-trafficking pathways are disrupted in ArpC3 cKO enterocytes

The foregoing characterizations did not reveal any obvious defects in ArpC3 cKO mice that could explain the growth arrest and lethality phenotypes. In addition to regulating cytoarchitecture and cortical F-actin, the Arp2/3 complex has been demonstrated to regulate vesicle trafficking (Rajan et al., 2009; Duleh and Welch, 2010, 2012). Much of this is through its activator WASH, and loss of WASH in cultured cells resulted in defects in the endolysosomal system (Derivery et al., 2009; Gomez and Billadeau, 2009; Gomez et al., 2012; Duleh and Welch, 2010). Analysis of ArpC3 cKO intestines by electron microscopy revealed a range of phenotypes, including extensive vesiculation and large inclusions (Supplemental Figure S2). This prompted us to examine the localization of proteins that label various vesicle populations to better understand whether trafficking pathways were disrupted upon loss of Arp2/3 complex activity.

The Arp2/3 complex has been reported to play roles in a number of vesicle-trafficking pathways, including invagination and pinching of endosomes and delivery to sorting endosomes (Stamnes, 2002; Martin et al., 2006; Duleh and Welch, 2010). We stained intestinal sections with antibodies against EEA1, an early endosomal marker, but did not find significant changes in its localization by light microscopy (Figure 3, A and B). We next immunostained for Vps26, a subunit of the retromer complex. This complex regulates the sorting of transmembrane cargo from endosomes to Golgi and the plasma membrane (Burd and Cullen, 2014). We were particularly interested in Vps26, as loss of the Arp2/3 activator, WASH, resulted in defective Vps26 localization (Gomez and Billadeau, 2009). In wild-type enterocytes, Vps26 localized most strongly to the very apical area and to the perinuclear region (Figure 3, C and C'). In the mutant intestine, Vps26 localized to larger and less uniform structures, and these extended further down toward the nucleus (Figure 3D). Quantitation revealed a significant number of cells with abnormal Vps26 staining (Figure 3E). Although the size of Vps26 particles was quite uniform in WT intestinal cells, there was a much larger size distribution in the mutant (Figure 3F). These results suggest that endosome sorting is impaired in ArpC3 cKO mice.

Disruption of vesicle sorting often leads to mistargeting of cargo to the lysosome. We examined this possibility by immunostaining with the lysosomal marker Lamp2. Lamp2 appeared in a diffuse crown at the apical region of most wild-type enterocytes (Figure 3, G and G'). In the ArpC3 cKO mice, Lamp2 was still detectable in the apical region, albeit with less regular morphology. Moreover, many mutant enterocytes contained large Lamp2 puncta (Figure 3, H, H', and I). To determine whether this phenotype was exacerbated with time, we isolated intestines from late P0 pups and examined Lamp2 immunostaining. Of interest, in some ArpC3 cKO cells, Lamp2 formed giant aggregates, whereas other cells completely lacked Lamp2 signal (Figure 3, J and K). This is in contrast to the wild type, in which Lamp2 appears uniformly at the apical region at all times.

IgG transcytosis is impaired in ArpC3 cKO mice

The foregoing results demonstrate that ArpC3 is required for some vesicle-trafficking pathways and that mutants develop lysosomal defects. We next wanted to investigate how this affects the transport of physiologically important biological molecules. Neonates have immature immune systems and receive immunoglobulins from their mother's milk. The IgG in milk is transcytosed through the enterocyte and released through the basolateral membrane (Rojas and Apodaca, 2002; Rath et al., 2013). The retromer is required for basolateral to apical transcytosis of the polymeric immunoglobulin receptor and IgA in hepatocytes (Verges et al., 2004), although its role

in apical-to-basolateral transcytosis has not been studied. Of note, the localization of the retromer component Vps26 was perturbed in ArpC3 cKO intestine. To date, a specific requirement for the Arp2/3 complex in transcytosis has not been reported. We began by examining the localization of endogenous IgG in either unfed neonates or those who had ingested their mother's milk. Intestinal sections were stained with fluorescently labeled anti-mouse secondary antibodies. In unfed mice (both wild type and ArpC3 cKO), we did not observe the presence of IgG within enterocytes (Figure 4, A and B). In wild-type pups that had fed, we observed small puncta at the apical side of the cell, consistent with their apical internalization and subsequent rapid transcytosis out of the cell (Figure 4, C and C'). In contrast, ArpC3-null enterocytes had a greater amount of IgG puncta in the apical region. These puncta existed in a range of sizes, and in some cells, large aggregates were apparent (Figure 4, D and E). This is consistent with a defect in the normal transport of internalized IgG.

We next determined whether exogenous IgGs were trafficked differently by mutant enterocytes. To this end, we performed a pulse chase experiment in which intestinal explants were exposed to IgG at 4°C to allow binding and then, after washing away excess IgG, raised the temperature to 37°C to allow internalization; samples were fixed and examined at 15- and 30-min time points. At 15 min, we saw internalization of fluorescent IgG at the apical surface of both WT and ArpC3 cKO intestine (Figure 4, F and G). This indicates that there was no defect in internalization in ArpC3 cKO intestines. At 30 min, the IgG was primarily localized at the basolateral region of the WT enterocytes. In contrast, the IgG remained at the apical region of ArpC3 cKOs, demonstrating a defect in the trafficking of this cargo (Figure 4, H and I). In controls for which no antibody was added, fluorescence signal was not detected within enterocytes (Supplemental Figure S3). Thus, the IgG transcytosis system is defective in ArpC3 cKO mice.

Lipid absorption is impaired in ArpC3 cKO jejunum

In addition to IgG transcytosis, the neonatal intestine must absorb nutrients, including lipids. The major components of dietary fat, including fats derived from milk, are triglycerides. These are broken down into monoglycerides and fatty acids, which are believed to diffuse into cells when present at high concentrations and to be transported in when their concentrations are lower (Lynes et al., 2011; Pepino et al., 2014). Once in the cell, these components are reassembled into triglycerides and lipoprotein particles, which are then released through the basolateral membrane. We used Oil Red O to stain jejunal sections and found a significant decrease in lipid accumulation in the mutant enterocytes (Figure 5, A and B). We quantitated this in two ways— by analyzing the size distribution of lipid puncta and by analyzing the total fluorescence intensity of Oil Red O staining within the enterocytes (Figure 5, C and D). By both measures, there was a clear defect in the mutant. In the duodenum, where lipid concentrations are highest, we did not note such a significant decrease, consistent with simple diffusion being sufficient for absorption at high lipid concentrations (Supplemental Figure S4).

We hypothesized that loss of ArpC3 might disrupt the localization of lipid transporters, such as CD36. Not only has CD36 been implicated in sensing and internalizing dietary lipids, but its internalization has been shown to be F-actin dependent (Nassir et al., 2007; Drover et al., 2008; Collins et al., 2009; Chevrot et al., 2012). In the neonatal gut, we found that CD36 clearly marked the apical surface of enterocytes of unfed wild-type and ArpC3 cKO pups (Figure 5, E and F). Therefore there is no evidence for an apical localization
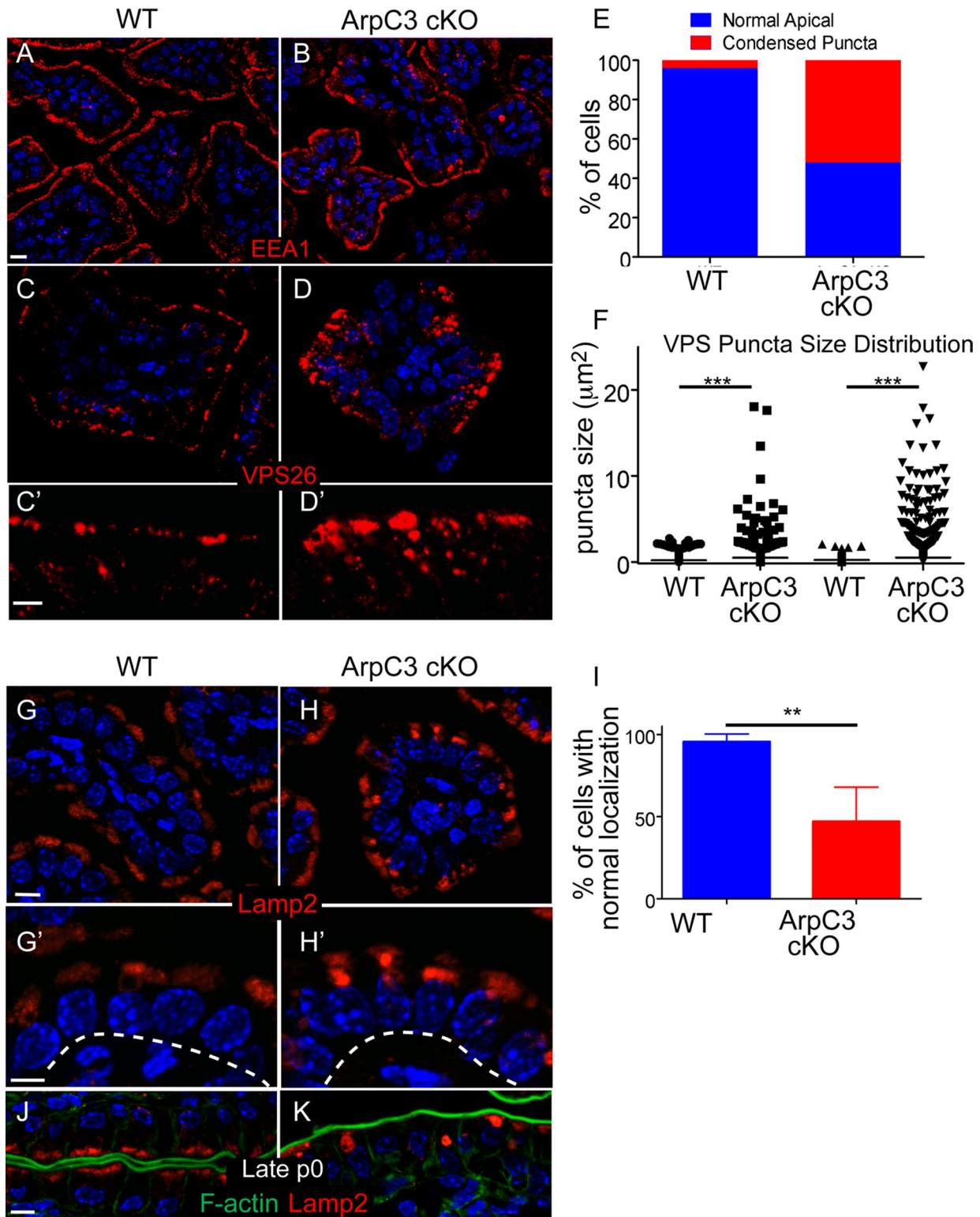
FIGURE 3: Defects in retromer and lysosomal pools in ArpC3 cKO intestines. WT and ArpC3 cKO intestines were stained with antibodies against the early endosomal marker EEA1 (red) (A,B) or with antibodies against the retromer subunit VPS26 (red) (C–D'). (C', D') Magnified views of the apical regions of the intestine. (E) Quantitation of the number of enterocytes with normal/abnormal VPS26 localization. Intestines from WT and mutant animals from two different litters were used for analysis; $p = 0.004$. (F) Quantitation of the size of VPS26 puncta from two distinct WT and ArpC3 cKO intestines. $p = 0.007$. (G–H') Staining for the lysosomal protein Lamp2 (red) in WT and ArpC3 cKO intestinal sections. (G', H') Higher-magnification views of the apical localization. Dashed lines indicate basement membranes. (I) Quantitation of cells with normal Lamp2 localization in WT and ArpC3 cKO intestines. Two mice for each genotype; $p < 0.01$. (J, K) Localization of Lamp2 (red) and F-actin (green) in intestines from neonates taken at late P0. Scale bars, 10 μm, except C', D', G', and H', 5 μm.
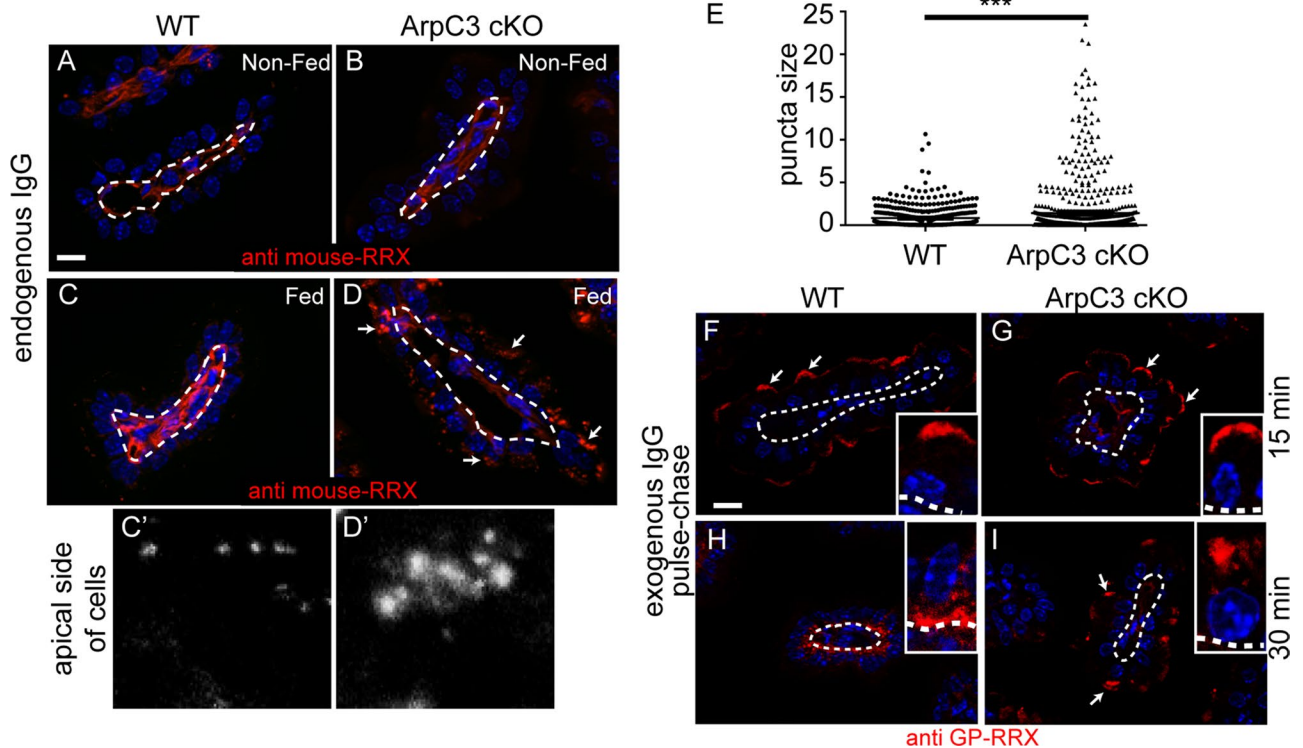
FIGURE 4: Transcytosis defects in ArpC3 cKO intestines. (A–D) Analysis of endogenous IgGs in WT and ArpC3 cKO intestines, as indicated. (A, B) Neonatal mice that had not suckled; (C, D) mice that had. Sections were stained with donkey anti-mouse antibodies labeled with Rhodamine Red-X to detect the presence of endogenous IgGs. Dashed lines indicate the basement membrane; arrows indicate apical puncta. (E) Quantitation of IgG puncta size. Two mice/genotype, $p = 0.0002$. (F–I) WT or ArpC3 cKO intestines, as indicated, were incubated with donkey anti–guinea pig-Rhodamine Red-X at 4°C for 15 min and then washed and incubated at 37°C. Samples were fixed after 15 (F, G) and 30 min (H, I), and then imaged. All insets are displayed with apical at the top and basal at the bottom, with the dashed line indicating the basement membrane. Scale bar, 10 μm. Arrows highlight apical puncta of IgG.

defect. Consistent with this, we found that both alkaline phosphatase and the glucose transporter SGLT1 localized normally to the apical domain (Supplemental Figure S5). However, we observed a dramatic internalization of CD36 in the intestines of fed WT mice (those exposed to milk and therefore lipids), as shown in Figure 5G. In contrast, this relocalization was completely lost in the ArpC3 cKO pups, and CD36 retained its apical localization (Figure 5H). This is despite the fact that they had clearly fed, as indicated by the presence of milk in the stomach and intestines (unpublished data). These data demonstrate that CD36 internalization is both a lipid- and an Arp2/3 complex–dependent phenomenon. Consistent with this, F-actin was detectable on internalized CD36 structures in fed wild-type mice (Figure 5I, a magnification of the boxed region in G). Although the mechanisms of lipid absorption are not fully understood, these data demonstrate an essential role for the Arp2/3 complex in regulating the internalization of a lipid transporter. We next asked whether this resulted in a change in the levels of plasma triglycerides. There was a wide biological range of triglyceride levels in the wild-type animals (ranging from 43 to >100 mg/dl). The ArpC3 cKO neonates, however, showed a statistically significant decrease in plasma triglyceride levels, with a mean around 25 mg/dl. Thus, failure to properly absorb and process lipids is likely one factor underlying the failure-to-thrive phenotype of the ArpC3 cKO mice.

DISCUSSION

In this study, we revealed for the first time some of the functions of the Arp2/3 complex in a simple mammalian epithelial tissue, the

small intestine. Our findings demonstrate that, surprisingly, ArpC3 is not required for the generation of the bulk of cortical F-actin, either apical or basolateral. However, Arp2/3 complex function is required for viability of the mice. Our data suggest that the essential roles of the Arp2/3 complex in the intestine are in organizing vesicle-trafficking pathways. Defects in the endolysosomal system are likely to lead to an array of defects, some of which we have documented here, including transcytosis and lipid absorption.

One of the surprising findings of this study was that there was no substantial decrease in cortical F-actin in the ArpC3 cKO mice. This is in contrast to loss of Arp2/3 complex activity in the *C. elegans* gut (Bernadskaya *et al.*, 2011). Consistent with this, the F-actin–binding protein ezrin was mislocalized in the *C. elegans* gut upon depletion of Arp2/3 complex, but ezrin localization was normal in the ArpC3 cKO mammalian gut, even though both of these are presumably strong hypomorphs. Although it remains possible that low levels of Arp2/3 complex activity are sufficient to generate cortical F-actin in the mammalian gut, our data suggest that other mechanisms exist to accomplish this in the absence of ArpC3. Although formins and other nucleators remain excellent candidates for this cortical F-actin–generating activity, it is also possible that it is mediated by de novo nucleation-independent mechanisms. Among the prominent functions of cortical F-actin are its roles in cell–cell adhesion structures. Consistent with the lack of observable change in F-actin organization, we did not detect any changes in the localization of adherens and tight junctions proteins. A great deal of work in vitro, in cultured cells and in the *Drosophila* notum, suggested important
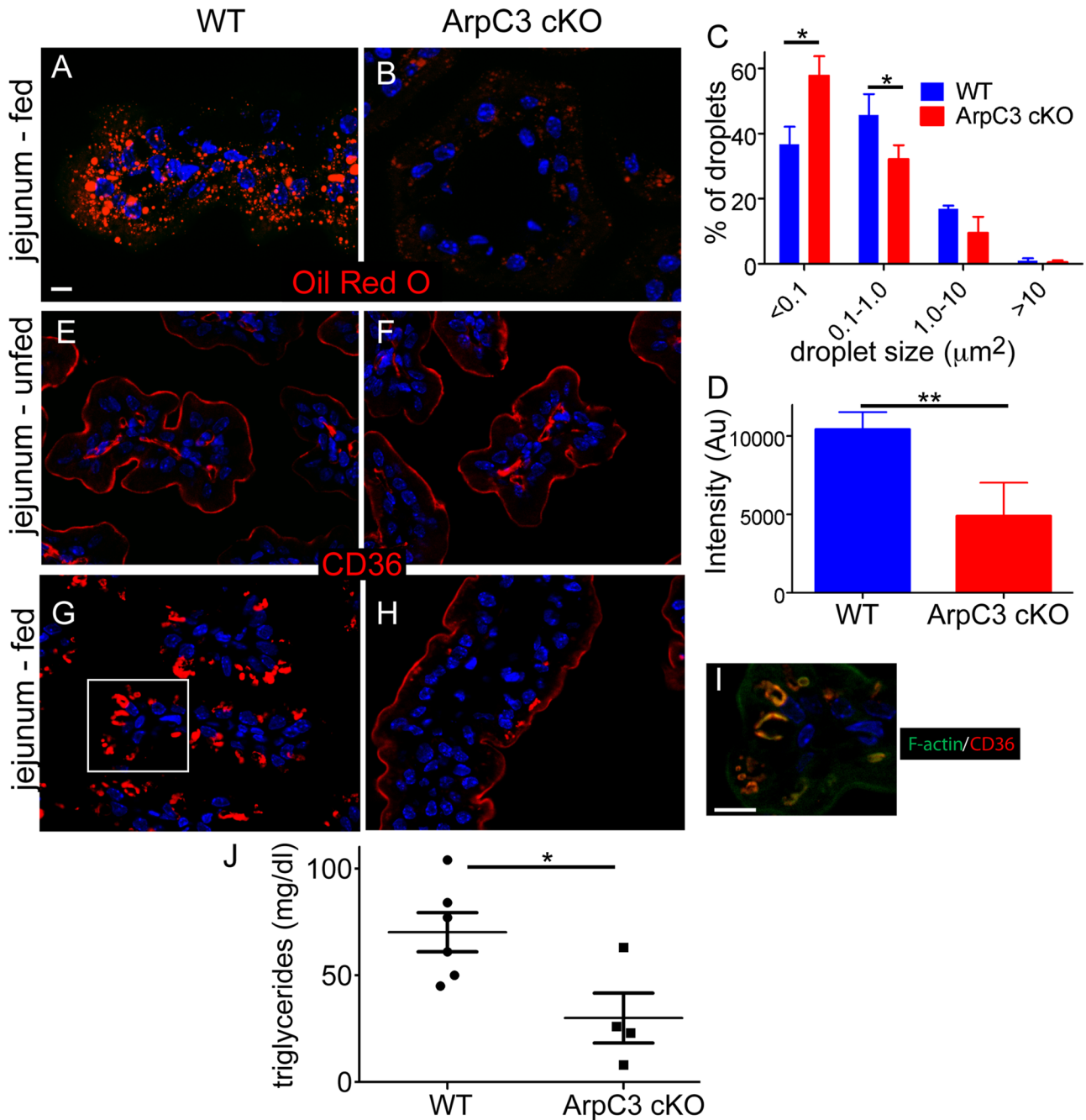
FIGURE 5: Defect in lipid uptake in the jejunum of the ArpC3 cKO mice. (A, B) Oil Red O staining of WT and ArpC3 cKO mice. Intestinal sections were from the jejunum. (C) Quantitation of sizes of Oil Red O particles in WT and ArpC3 cKO intestine. $p = 0.01$ for <0.1 μm and 0.03 for 0.1–1.0 μm. D. Quantitation of total intensity of Oil Red O fluorescence in WT and ArpC3 cKO enterocytes. $p < 0.01$. (E–H) CD36 localization in unfed (E, F) and fed (G, H) intestines. (I) The boxed region in G with F-actin (green) costain. (J) Quantitation of plasma triglyceride levels in WT and ArpC3 cKO neonates ($p < 0.05$).

roles for the Arp2/3 complex in assembling junctional F-actin and promoting proper adherens junction morphology (Verma et al., 2004, 2012; Georgiou et al., 2008; Tang and Brieher, 2012). Recent data, however, suggest that this might be most important for generating junctional tension (Verma et al., 2012). Consistent with this, we did see defects in apical membrane organization in a small subset of ArpC3 cKO villi.

The Arp2/3 complex does not appear to be essential for bulk endocytosis or apical membrane identity in enterocytes. IgG was efficiently internalized in mutant cells, and the apical localization of

a number of brush border proteins was normal (such as alkaline phosphatase and SGLT1). Despite this, specific defects were noted in CD36 internalization in the intestinal jejunum. CD36's internalization has been demonstrated to be F-actin dependent in T-cells, and our work demonstrates that it is Arp2/3 complex dependent in enterocytes (Collins et al., 2009). CD36 endocytosis is believed to internalize free fatty acids (Nassir et al., 2007; Drover et al., 2008; Pepino et al., 2014). Although this system is not required at high lipid levels, such as those seen in the duodenum of neonates fed a high-fat milk diet, it is believed to mediate internalization at lower

lipid concentrations. Consistent with this, we noted a specific internalization of CD36 in the jejunum that had been exposed to fat. CD36 was not internalized when cells were not exposed to lipid (unfed), and it was not internalized in the absence of the Arp2/3 complex. This is physiologically significant, as mutant mice have decreased plasma triglyceride levels. These data suggest a selective function for Arp2/3 complex in the endocytic internalization of some cargo. Future work to identify differences in brush border architecture using proteomics may reveal a subset of physiologically relevant proteins that require the Arp2/3 complex for internalization and/or apical localization.

The mechanisms underlying transcytosis of IgG across enterocytes remain incompletely understood. An apical membrane receptor, FcRn, binds IgG, and this complex is subsequently internalized (Rojas and Apodaca, 2002; Rath et al., 2013). This does not require Arp2/3 complex function, as both exogenous and endogenous IgGs were taken up by mutant intestinal epithelial cells. However, once internalized, IgG needs to be targeted to the basolateral membrane. This process does require Arp2/3 complex, and, in its absence, IgG accumulated in the cell. The proteins involved in sorting have not yet been described, although the retromer complex is required for basolateral-to-apical transcytosis (Verges et al., 2004). Retromer localization is disrupted in the ArpC3 cKO intestine, making it an important candidate in IgG trafficking. It remains unclear whether the Arp2/3 complex has a specific role in the trafficking of IgG or whether general disruption of vesicular organization is perturbed and thus transcytosis is indirectly affected. However, the normal localization of other apical and lateral membrane proteins suggests that only specific pathways are disrupted.

An outstanding question is how loss of Arp2/3 complex activity results in broad vesicle- trafficking defects. Although there could be structural defects (i.e., cytoplasmic F-actin scaffolds that are required for tubulation, scission, and vesicle movement events) underlying these phenotypes, there is some selectivity that suggests more complex mechanisms. Of note, the defects seen are consistent with those in cells with perturbed WASH or retromer function (Derivery et al., 2009; Gomez and Billadeau, 2009; Gomez et al., 2012; Burd and Cullen, 2014). Thus Arp2/3 complex is likely to have important functions at sorting endosomes directing specific cargoes to different sites. This is consistent with the transcytosis and lysosomal defects that we observed. Of note, not all cargoes are retromer dependent, and we have seen normal localization of a number of apical and basolateral proteins (Nisar et al., 2010). Although additional vesicle-trafficking pathways may be affected, it is also possible that disruption of this single pathway could result in many of the downstream effects we observed. Further work is required to determine whether vesicle motility and/or specific tubulation or scission or scission events are disrupted.

In conclusion, our work has demonstrated that in an intact mammalian tissue—the small intestine—the Arp2/3 complex has rather specific functions in organizing some vesicular trafficking pathways. This results in physiological defects in the uptake of two important biological molecules—IgGs and lipids. Further analysis is likely to define additional proteins/pathways that rely on Arp2/3 complex function for their proper localization and function.

MATERIALS AND METHODS
Mice
Villin-Cre and ArpC3 fl/fl mice have been described previously (Madison et al., 2002; Kim et al., 2013). All mouse studies were performed with approval from the Institutional Animal Care and Use Committee of Duke University.

Immunofluorescence staining and histology
Unless specified, the middle region (jejunum) of small intestine from P0 pups was cut into 0.5- cm pieces, flushed with 1× Hank's balanced salt solution (HBSS) buffer, and fixed with 4% (wt/vol) paraformaldehyde either for 3 h at room temperature or overnight at 4°C. After three washes with cold 1× phosphate-buffered saline (PBS) buffer, tissues were cryoprotected with 30% sucrose in Tris-buffered saline buffer at 4°C and immersed in OCT:30% sucrose at a ratio of 2:1 for 30 min before freezing at –80°C. Ten-micrometer-thick tissue sections were permeabilized with PBST (0.1% Triton X-100 in PBS) and then blocked with PBST containing 5% (wt/vol) normal goat serum, 5% (wt/vol) normal donkey serum, and 3% (wt/vol) bovine serum albumin (Sigma-Aldrich, St. Louis, MO; goat serum was omitted when goat antibodies were used). MOM block (Vector Labs, Burlingame, CA) was used when staining mouse tissue with mouse antibodies. Antibodies used included goat anti-Myo1d (Santa Cruz Biotechnology, Dallas, TX), rabbit anti-Par3 (Upstate, Billerica, MA), rabbit anti-ZO1 (Invitrogen, Carlsbad, CA), rabbit anti-EEA1, rabbit anti-Vps26, rabbit anti-Ki67, mouse anti-Ezrin (Abcam, Cambridge, MA), rabbit ant–active caspase3, goat anti-CD36 (R&D Systems, Minneapolis, MN), rabbit anti-Lamp2 (Developmental Studies Hybridoma Bank, University of Iowa, Iowa City, IA), and rat anti-E-cadherin (from Colin Jamora, InStem, Bangalore, India). Secondary antibodies were Alexa 488 labeled (Invitrogen) or Rhodamine Red-X labeled (Jackson ImmunoResearch, West Grove, PA). F-actin was stained with Alexa 488– phalloidin (Invitrogen). Images were acquired with an Axio Imager Z1 microscope with Apotome attachment (Zeiss, Thornwood, NY).

Ten-micrometer sections were stained with Mayer's hematoxylin (Sigma-Aldrich) and eosin. To detect goblet cells, slides were stained with Alcian blue (1% Alcian blue in 3% acetic acid solution) for 10 min.

IgG uptake assay
For the pulse chase experiments, intestinal tissue fragments were incubated with 1× HBSS buffer containing fluorescently labeled IgG (donkey anti–guinea pig, 0.1 mg/ml) for 15 min on ice. After washing with cold 1× HBSS buffer, samples were placed in IgG-free buffer and shifted to 37°C for 15 or 30 min before being fixed with 4% paraformaldehyde. For the experiment with no chase, samples were incubated with labeled IgG, as described, at 37°C for 1 h and washed with 1× PBS three times before being fixed with 4% (wt/vol) paraformaldehyde overnight at 4°C. To analyze endogenous IgG uptake, we isolated intestines from P0 pups that had fed from their mothers (identified by the presence of a milk spot). Tissue sections were directly subjected to either Alexa 488–labeled goat anti-mouse or Rhodamine Red-X–labeled donkey anti-mouse antibodies without MOM blocking.

Oil Red O staining
Oil Red O stock solution was prepared by dissolving 500 mg Oil Red O in 60% triethylphosphate. Before use, a 36% working solution was filtered. Tissue sections were washed with deionized water and stained for 30 min at room temperature. After rinsing with deionized water three times and running tap water for 2 min, sections were labeled with Hoechst in 1× PBS for 1 min. Ten percent glycerol in PBS was used to mount the slide.

Western blotting
P0 pups were killed, and the jejunum was cut into 1-cm pieces and cut open. Tissue fragments were collected into a 1.5-ml Eppendorf tube containing 1× HBSS, 20 mM EDTA (Sigma-Aldrich), and 10 µM

Y27632 (SelleckChem, Houston, TX). The samples were incubated at 37°C for 6 min and then shaken for 30 s. The remaining tissue fragments were removed, and the tubes were centrifuged at 2400 rpm. The pellets were washed with cold HBSS and dissolved in 3× SDS sample buffer. Rabbit anti-ArpC3 (Santa Cruz Biotechnology) and mouse anti–β-actin (Sigma-Aldrich) were used for detection.

Plasma triglyceride analysis

Plasma was generated from blood collected from neonates on the afternoon after their birth. Triglyceride levels were determined using a Triglyceride Assay Kit (Cayman, Ann Arbor, MI).

REFERENCES

Bernadskaya YY, Patel FB, Hsu HT, Soto MC (2011). Arp2/3 promotes junction formation and maintenance in the Caenorhabditis elegans intestine by regulating membrane association of apical proteins. Mol Biol Cell 22, 2886–2899.

Burd C, Cullen PJ (2014). Retromer: a master conductor of endosome sorting. Cold Spring Harb Perspect Biol 6, a016774.

Chevrot M, Martin C, Passilly-Degrace P, Besnard P (2012). Role of CD36 in oral and postoral sensing of lipids. Handbk Exp Pharmacol 2012, 295–307.

Collins RF, Touret N, Kuwata H, Tandon NN, Grinstein S, Trimble WS (2009). Uptake of oxidized low density lipoprotein by CD36 occurs by an actin-dependent pathway distinct from macropinocytosis. J Biol Chem 284, 30288–30297.

Derivery E, Sousa C, Gautier JJ, Lombard B, Loew D, Gautreau A (2009). The Arp2/3 activator WASH controls the fission of endosomes through a large multiprotein complex. Dev Cell 17, 712–723.

Drover VA, Nguyen DV, Bastie CC, Darlington YF, Abumrad NA, Pessin JE, London E, Sahoo D, Phillips MC (2008). CD36 mediates both cellular uptake of very long chain fatty acids and their intestinal absorption in mice. J Biol Chem 283, 13108–13115.

Duleh SN, Welch MD (2010). WASH and the Arp2/3 complex regulate endosome shape and trafficking. Cytoskeleton 67, 193–206.

Duleh SN, Welch MD (2012). Regulation of integrin trafficking, cell adhesion, and cell migration by WASH and the Arp2/3 complex. Cytoskeleton 69, 1047–1058.

Firat-Karalar EN, Welch MD (2011). New mechanisms and functions of actin nucleation. Curr Opin Cell Biol 23, 4–13.

Galletta BJ, Cooper JA (2009). Actin and endocytosis: mechanisms and phylogeny. Curr Opin Cell Biol 21, 20–27.

Georgiou M, Marinari E, Burden J, Baum B (2008). Cdc42, Par6, and aPKC regulate Arp2/3-mediated endocytosis to control local adherens junction stability. Curr Biol 18, 1631–1638.

Gomez TS, Billadeau DD (2009). A FAM21-containing WASH complex regulates retromer-dependent sorting. Dev Cell 17, 699–711.

Gomez TS, Gorman JA, de Narvajas AA, Koenig AO, Billadeau DD (2012). Trafficking defects in WASH-knockout fibroblasts originate from collapsed endosomal and lysosomal networks. Mol Biol Cell 23, 3215–3228.

Gournier H, Goley ED, Niederstrasser H, Trinh T, Welch MD (2001). Reconstitution of human Arp2/3 complex reveals critical roles of individual subunits in complex structure and activity. Mol Cell 8, 1041–1052.

Kim IH, Racz B, Wang H, Burianek L, Weinberg R, Yasuda R, Wetsel WC, Soderling SH (2013). Disruption of Arp2/3 results in asymmetric structural plasticity of dendritic spines and progressive synaptic and behavioral abnormalities. J Neurosci 33, 6081–6092.

Lynes M, Narisawa S, Millan JL, Widmaier EP (2011). Interactions between CD36 and global intestinal alkaline phosphatase in mouse small intestine and effects of high-fat diet. Am J Physiol Regulatory Integr Comp Physiol 301, R1738–1747.

Madison BB, Dunbar L, Qiao XT, Braunstein K, Braunstein E, Gumucio DL (2002). Cis elements of the villin gene control expression in restricted domains of the vertical (crypt) and horizontal (duodenum, cecum) axes of the intestine. J Biol Chem 277, 33275–33283.

Martin AC, Welch MD, Drubin DG (2006). Arp2/3 ATP hydrolysis-catalysed branch dissociation is critical for endocytic force generation. Nat Cell Biol 8, 826–833.

McConnell RE, Higginbotham JN, Shifrin DA Jr, Tabb DL, Coffey RJ, Tyska MJ (2009). The enterocyte microvillus is a vesicle-generating organelle. J Cell Biol 185, 1285–1298.

Nassir F, Wilson B, Han X, Gross RW, Abumrad NA (2007). CD36 is important for fatty acid and cholesterol uptake by the proximal but not distal intestine. J Biol Chem 282, 19493–19501.

Nisar S, Kelly E, Cullen PJ, Mundell SJ (2010). Regulation of P2Y1 receptor traffic by sorting Nexin 1 is retromer independent. Traffic 11, 508–519.

Pepino MY, Kuda O, Samovski D, Abumrad NA (2014). Structure-function of CD36 and importance of fatty acid signal transduction in fat metabolism. Annu Rev Nutr 34, 281–303.

Pollard TD (2007). Regulation of actin filament assembly by Arp2/3 complex and formins. Annu Rev Biophys Biomol Struct 36, 451–477.

Rajan A, Tien AC, Haueter CM, Schulze KL, Bellen HJ (2009). The Arp2/3 complex and WASp are required for apical trafficking of Delta into microvilli during cell fate specification of sensory organ precursors. Nat Cell Biol 11, 815–824.

Rath T, Kuo TT, Baker K, Qiao SW, Kobayashi K, Yoshida M, Roopenian D, Fiebiger E, Lencer WI, Blumberg RS (2013). The immunologic functions of the neonatal Fc receptor for IgG. J Clin Immunol 33, (Suppl 1), S9–S17.

Rojas R, Apodaca G (2002). Immunoglobulin transport across polarized epithelial cells. Nat Rev Mol Cell Biol 3, 944–955.

Rotty JD, Wu C, Bear JE (2013). New insights into the regulation and cellular functions of the ARP2/3 complex. Nat Rev Mol Cell Biol 14, 7–12.

Saotome I, Curto M, McClatchey AI (2004). Ezrin is essential for epithelial organization and villus morphogenesis in the developing intestine. Dev Cell 6, 855–864.

Stamnes M (2002). Regulating the actin cytoskeleton during vesicular transport. Curr Opin Cell Biol 14, 428–433.

Tang VW, Brieher WM (2012). alpha-Actinin-4/FSGS1 is required for Arp2/3-dependent actin assembly at the adherens junction. J Cell Biol 196, 115–130.

Tyska MJ, Mackey AT, Huang JD, Copeland NG, Jenkins NA, Mooseker MS (2005). Myosin-1a is critical for normal brush border structure and composition. Mol Biol Cell 16, 2443–2457.

Tyska MJ, Mooseker MS (2004). A role for myosin-1A in the localization of a brush border disaccharidase. J Cell Biol 165, 395–405.

van Es JH, van Gijn ME, Riccio O, van den Born M, Vooijs M, Begthel H, Cozijnsen M, Robine S, Winton DJ, Radtke F, Clevers H (2005). Notch/gamma-secretase inhibition turns proliferative cells in intestinal crypts and adenomas into goblet cells. Nature 435, 959–963.

Verges M, Luton F, Gruber C, Tiemann F, Reinders LG, Huang L, Burlingame AL, Haft CR, Mostov KE (2004). The mammalian retromer regulates transcytosis of the polymeric immunoglobulin receptor. Nat Cell Biol 6, 763–769.

Verma S, Han SP, Michael M, Gomez GA, Yang Z, Teasdale RD, Ratheesh A, Kovacs EM, Ali RG, Yap AS (2012). A WAVE2-Arp2/3 actin nucleator apparatus supports junctional tension at the epithelial zonula adherens. Mol Biol Cell 23, 4601–4610.

Verma S, Shewan AM, Scott JA, Helwani FM, den Elzen NR, Miki H, Takenawa T, Yap AS (2004). Arp2/3 activity is necessary for efficient formation of E-cadherin adhesive contacts. J Biol Chem 279, 34062–34070.

Winter DC, Choe EY, Li R (1999). Genetic dissection of the budding yeast Arp2/3 complex: a comparison of the in vivo and structural roles of individual subunits. Proc Natl Acad Sci USA 96, 7288–7293.

Zhou K, Muroyama A, Underwood J, Leylek R, Ray S, Soderling SH, Lechler T (2013). Actin-related protein2/3 complex regulates tight junctions and terminal differentiation to promote epidermal barrier formation. Proc Natl Acad Sci USA 110, E3820–E3829.